

Article

Variable-Speed Propeller Turbine for Small Hydropower Applications

Eva Bílková ^{1,*} , Jiří Souček ¹ , Martin Kantor ² , Roman Kubíček ³ and Petr Nowak ¹

¹ Hydraulic Structures Department, Faculty of Civil Engineering, Czech Technical University, 166 29 Prague, Czech Republic

² Institute of Machines and Power Engineering, Faculty of Mechanical Engineering, University J. E. Purkyně, 400 96 Ústí nad Labem, Czech Republic

³ Elzaco spol. s r.o., 787 01 Šumperk, Czech Republic

* Correspondence: eva.bilkova@fsv.cvut.cz; Tel.: +420-224-354-666

Abstract: Standard technical solutions are not cost-effective for many small hydropower sites. This study aims to demonstrate the workflow for the tailor-made variable-speed axial propeller turbine and provide proof of this concept. The turbine is designed to meet the site's specific space limitations and operating range needs. The runner shape is adjusted to the variable-speed operation and defined hydraulic profile using a parametric geometry model and CFD-based optimization. The variable-speed propeller turbine shows excellent flow control while keeping the mechanical design simple. The tailor-made approach minimizes construction costs using existing structures and is highly suitable for mini-hydropower applications. The prototype—an atypical turbine designed for highly restricted space and installed on-site—serves as proof of the concept. The findings on the design of axial variable-speed turbines are presented.

Keywords: axial propeller turbine; variable-speed; optimization; tailor-made design; CFD; CAESSES



Citation: Bílková, E.; Souček, J.; Kantor, M.; Kubíček, R.; Nowak, P. Variable-Speed Propeller Turbine for Small Hydropower Applications. *Energies* **2023**, *16*, 3811. <https://doi.org/10.3390/en16093811>

Academic Editors: Bernhard Semlitsch and Christian Bauer

Received: 23 February 2023

Revised: 12 April 2023

Accepted: 25 April 2023

Published: 28 April 2023



Copyright: © 2023 by the authors. Licensee MDPI, Basel, Switzerland. This article is an open access article distributed under the terms and conditions of the Creative Commons Attribution (CC BY) license (<https://creativecommons.org/licenses/by/4.0/>).

1. Introduction

Hydropower has been a source of electric energy since the end of the 19th century. Although a large part of the EU hydropower potential is already used, there are still steady investments in hydropower, and the installed capacity is continuously increasing [1]. Additionally, upgrading, uprating, and renovating older power stations is an opportunity to significantly increase their efficiency and flexibility and reduce operation and maintenance costs [2].

This paper focuses on technology mini- and micro-hydro sites whose potential lies in a large number of various sites, including drinking water and irrigation networks, dam bottom outlets, and old mill sites. Its harnessing does not have any environmental impact and can be economically significant for the operator.

However, the state of existing technologies limits the hydro-energetic use of those sites, especially with installed power below 50 kW. Energy potential is often not exploited at all or only with low efficiency. Standard technical solutions are often not cost-effective due to high investment costs (Kaplan turbine), low efficiency (PAT [3]), or low specific speed (water wheels [4], hydrodynamic screw [5]). Although the peak efficiency of these technologies can exceed 80%, the global efficiency is significantly lower (50–70%) [2]. Using standardized solutions (as a PAT series) usually further reduces the overall energy production as it is hard to precisely match the location's needs due to the extreme variability of the sites.

To cover the described technology gap, we propose the concept of a tailor-made variable-speed turbine that is designed and optimized for each site to meet its specific demands. Variable-speed technology has been under intense research recently, mainly for large reversible turbines [6]. Valavi et al. [6] and Iliev et al. [7] summarized the state of the art of the variable-speed Francis turbine in their reviews. They describe a significant research

gap in the shape optimization of variable-speed turbines. Iliev et al. [8] subsequently published work about hydraulic shape optimization of the Francis turbine for variable speed operation using a surrogate model.

Although the mentioned reviews were referring mainly to Francis turbines, a more extensive review on the use of variable-speed axial turbines has not yet been published at all.

One of the first assessments of variable-speed operation of the axial turbines was made by Farrel et al. [9] in 1987. Relations were derived from the Euler equation and other analytical equations. Farell described the connection between the relative blade spacing T/l (ratio of the blade spacing T to blade chord length l) and the flow control potential by varying the runner speed. Verifying this assumption without extensive modeling was extremely difficult.

Farell states that the larger the relative blade spacing T/l (less or shorter blades), the flatter the flow as a function of speed, which is unfavorable for variable-speed operation. It is also estimated that the flow control capability of the turbine increases with its higher specific speed.

About 25 years later, Borkowski [10,11] showed that a variable-speed propeller (or semi-Kaplan) turbine is a suitable solution for small hydro applications. This concept simplifies the mechanical design of the turbine and extends its operational range. Borkowski focuses mainly on the concept of electrical and control parts. Optimizing the hydraulic shape of the turbine is not part of the published works.

Recently, Barsi et al. [12] have contributed to the hydraulic design of axial variable-speed turbine research. The published work investigates the relationship between guide vanes' position and operating range. The shape optimization is not considered.

This paper extends previous research and focuses on the hydraulic design of axial variable-speed propeller turbines suitable for low-head mini- and micro-hydro applications. The presented workflow enables us to design a tailor-made turbine individually for each site, which is particularly advantageous for sites with existing structures.

The parametric geometry modeling, CFD, and automated shape optimization were used to meet the location's specific space requirements and operating range needs. This paper illustrates the workflow and models using data related to the Podhora SHPP, which served as a proof-of-concept.

2. Materials and Methods

2.1. Design Workflow

The proposed workflow adapts the hydraulic design to the structure's spatial possibilities and other functions. The maximal use of the existing constructions and technology minimizes investment costs and realization time. This results in a cost reduction not only for the construction but also on the formal side of the project, as much less administration is usually required. The money and effort saved can be used to optimize the shape of the turbine and increase its efficiency.

The design workflow assumes that the hydraulic profile of the turbine would be aligned with the spatial and operational requirements. A specially designed runner compensates for the compromised shape of the meridional profile. It is optimized directly for the given hydraulic conditions to achieve high efficiency and the required flow operating range. Figure 1 shows a complete workflow overview.

In the first step, a detailed survey of water management and the current state of structures is crucial as the tailor-made design uses the maximum of existing structures. A simple 3D scan by a depth camera or lidar technology is ideal. The resulting spatial model, including all details as control mechanisms, complements the documentation (if any is available) and is the base for preparing the spatial model of the design.

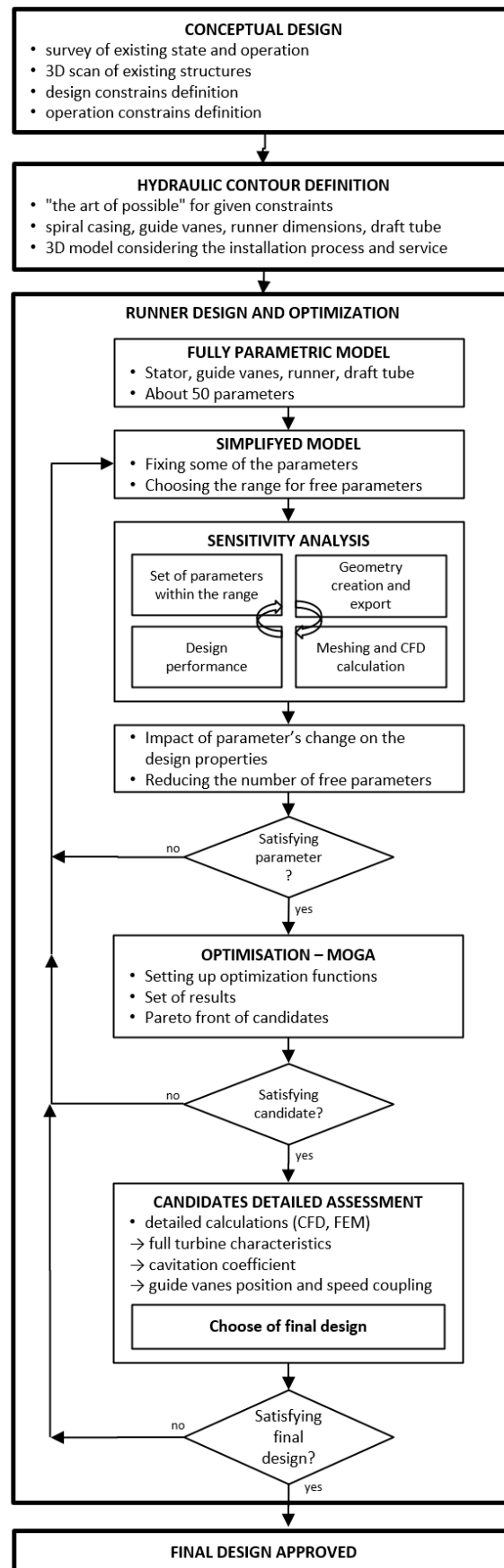


Figure 1. The design and optimization workflow.

In the second step, the position of the turbine and generator is designed, and the meridional hydraulic contour is defined. The shape of the individual turbine part is adjusted to space constraints and the installation process. The detailed spatial geometry model shown in Figure 2 prevents any conflict during installation or maintenance. The Rhino 3D modeler [13] (commercial software, McNeel Europe, Rhino 7) was used in the presented work.

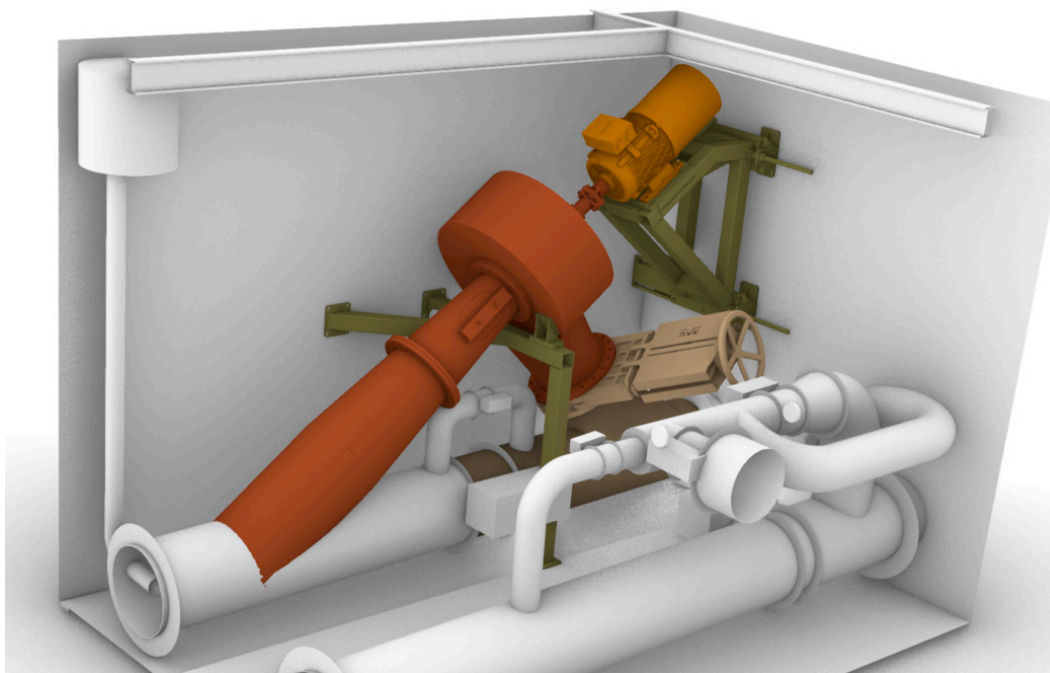


Figure 2. A spatial model of the Podhora SHPP—position of the turbine and generator defined, conflicts during installation avoided, meridional profile defined, and waiting for the runner design.

Once the meridional profile is defined, the turbine runner can be designed and optimized. This is a crucial point of the whole process and will be described in detail in Section 2.4. Finally, a thorough assessment of the promising candidates that emerged from the optimization process is carried out. The detailed model verifies the simplified calculations used for shape optimization. Furthermore, it provides an essential input for a detailed design, such as force and moment load (for mechanical and electrical design) or the optimal coupling of runner speed and guide vanes position (for controlling system design).

2.2. Technical Concept

The presented concept of the axial propeller turbine with variable-speed operation simplifies the mechanical design to reduce investment and maintenance costs while keeping the benefits of double regulation. Adjustable guide vanes control the flow direction to the runner and serve as an operation gate that closes the flow. The variable-speed operation, described in detail in Section 2.3, provides the second regulation. The concept was thoroughly presented by Borkowski [10]. Varying the rotational speed improves adaptation to the changing head and discharge and increases overall efficiency.

The propeller runner has no adjusting mechanism of the blades, which is mechanically the most challenging part of the Kaplan turbine. Design with the fixed runner blades simplifies the manufacturing process and opens new possibilities, such as CNC milling the runner from one piece (applicable for small diameters). The simple cylindrical runner chamber (thick-walled pipe) can be used instead of the technically complicated spherical chamber.

The electrical part consists of an induction or permanent magnet generator (PMG) and four-quadrant frequency converter. PMG is highly suitable for low-speed, high-torque, directly driven units. Standard induction generators can be installed in higher-speed

applications. The maximum torque of the variable-speed turbine does not correspond to the maximum power operating point. Therefore, a CFD study must deliver turbine torque-speed characteristic. The generator and frequency converter must be designed following this characteristic, not to exceed voltage, current, frequency, torque, speed, and heat loss limits.

The more complex concept of the electric part brings some important side benefits. When designing, there is no need to keep a fixed turbine speed or to use a gearbox [10]. The frequency converter allows the soft start/stop of the machine (to avoid inrush currents) and continuous power factor control and can avoid operating under unstable or cavitation conditions of the turbine.

2.3. Variable-Speed Operation

The existing literature does not sufficiently cover the design and optimization of variable-speed axial turbines. However, controlling the proposed Semi-Kaplan turbine with a fixed runner is analogous to the Francis turbine, and therefore, some of the knowledge can be used.

Fixed-speed Francis turbines are designed for a single operating point defined by the head, flow rate range, and runner rotational speed. If the head or flow rate changes out of a limited range, the machine's efficiency drops and problems with cavitation and pressure pulsations occur [6]. When operated out of the optimum, the residual vortex rotates in the draft tube around the machine axis in the direction of runner rotation ($Q < Q_{BEP}$) or against it ($Q > Q_{BEP}$). That leads to a reduction in turbine efficiency and other unfavorable phenomena. Adjusting the runner rotation speed eliminates vortex creation [7].

The semi-Kaplan turbine's behavior over the operational range is comparable. Drtina [14] states that the residual water rotation leaving the runner affects the draft tube performance. As a large part of the losses of a low-head turbine is induced in the draft tube, the residual rotation significantly affects the turbine's overall efficiency. Adjusting the rotation speed broadens the semi-Kaplan turbine's operation range, as shown in Figure 3.

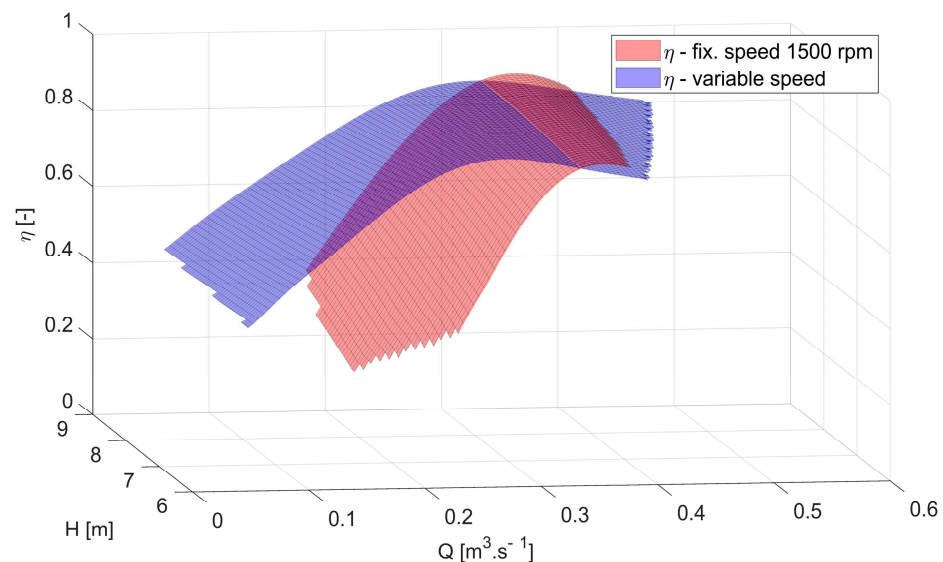


Figure 3. Operating range comparison—fixed speed vs. variable-speed operation of a propeller turbine considering the efficiency of a frequency converter.

When designing a variable-speed turbine, the following aspects must be considered [6]:

- Atypical hydraulic design;
- Increased risk of resonance in the system due to the operating speed range;
- The space required for the frequency converter and cooling;
- The more complicated layout of the electrical part.

Iman-Eini et al. [15] analyzed additional losses due to variable-speed operation in detail. The total losses consist of generator, mechanical, converter, and filter losses. These losses reduce the unit's power output and result in higher cooling requirements. By designing the best efficiency point near the synchronous speed, the turbine can be operated directly connected to the grid without speed control and related losses at this point [7].

Variable-speed operation in small hydropower plants has been tested on several prototypes with various technical arrangements [2,11,16,17].

2.4. Runner Design

The shape of the efficiency characteristic strongly influences the benefit of the variable-speed operation. The hydraulic shape of the turbine should therefore be designed and optimized specifically for variable-speed operation. However, the guidelines for variable-speed axial turbines have yet to be described in detail.

2.4.1. Parametric Geometry Model

The design of conventional turbines described in the literature [18] must be modified for variable-speed turbines. However, it can be efficiently used for the initial design that will be further optimized for variable-speed operation [7].

The fully parametric geometry of the axial propeller turbine in the size of the prototype (runner diameter of 0.27 m) was created in the CAESSES modeler [19] (commercial software, Friendship Systems). The CAESSES modeler was initially developed for ship design optimization [20,21] and copes well with smooth hydraulic shapes. Recently, a wide range of features for turbomachinery design was added.

The initial design was based on the standard propeller turbine design rules. The spatial requirements predefined the shape of the meridional profile. The guide vanes had a simple shape created by sweeping a predefined profile and were not subject to optimization in this work.

The conceptual design defines the number of blades and shroud contour. The hub contour can be slightly modified during optimization. The shape of the conical hub and the height of the runner chamber are defined by two free parameters.

The crucial part of the model is the runner blade definition. The 2D profiles in developed cylindrical sections, as shown in Figure 4a, are used to define the blade. The camber-based profile with symmetrical thickness distribution is defined by two values—camber area and thickness function area. Subsequently, the profile is scaled by chord length and transformed to the proper position in the cylindrical section that is defined by angle Beta.

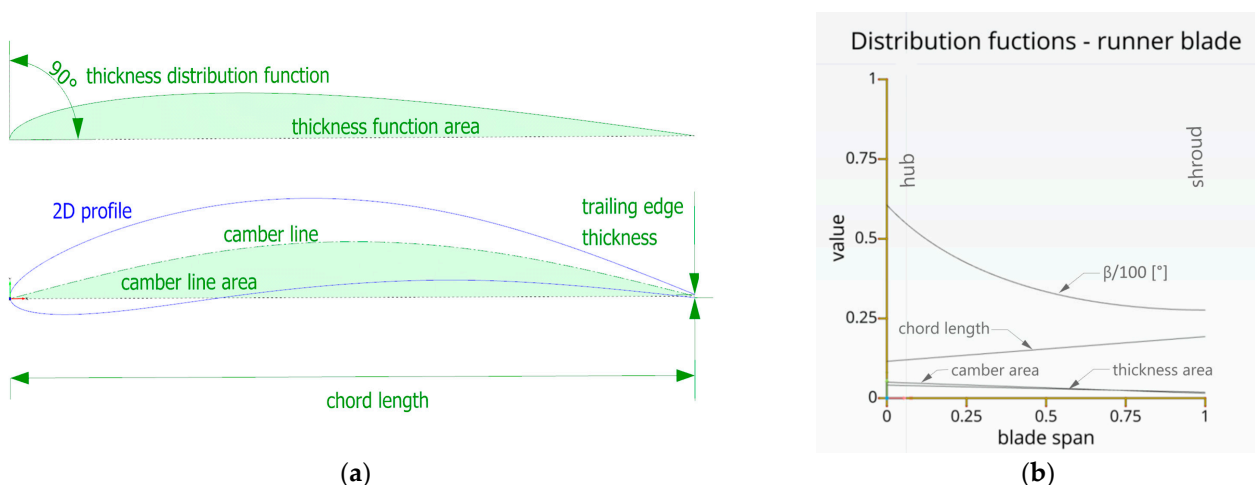


Figure 4. Parametric definition of the blade: (a) 2D profile definition; (b) distribution functions.

The distribution functions shown in Figure 4b express these values as a function of the relative blade span. Ten parameters define the distribution functions. Its shape, and

therefore the shape of the blade, is subject to optimization. The presented parametrization benefit is a low number of parameters, but it provides only limited options for varying the shape of profiles. More complex blade parametrization was presented by Kantor [22] using individual profile points or Kyriacou [23] using Bezier curves.

The position of the blade within the meridional profile is given by the stacking axis defined by two parameters. Another parameter controls the position of the guide vanes. The presented model had fifteen free parameters in total.

2.4.2. CFD Analysis

The created designs are assessed by CFD analysis in the commercial software Ansys CFX 21.1, which uses the finite volume method to solve incompressible RANS equations completed by the SST turbulence model [24].

Reducing the calculation time of one operation point is necessary to make the optimization process efficient. A steady-state analysis of the section model with one blade passage was used to reduce the number of computational elements, as shown in Figure 5a. The General Grid Interface type “Stage” (also called Mixing Plane) [25] was used to model the interface between stationary and rotating domains. The entire conical draft tube is included in the CFD analysis, and an idealized inlet vector replaces the spiral casing. Total Pressure is used at the inlet boundary and Averaged Static Pressure at the outlet boundary. Shroud tip clearance was neglected for the initial part of the optimization. In the final stage of the optimization and the characteristic calculation, the shroud tip clearance was considered.

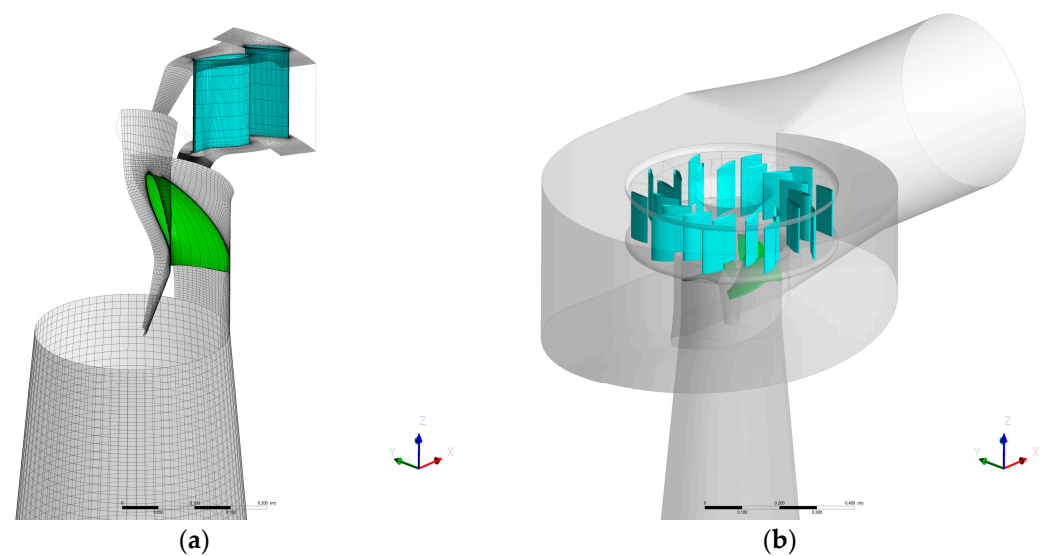


Figure 5. Model for numerical simulation. (a) The sectional model used for optimization. (b) Model of the full turbine with spiral casing used for the turbine characteristics calculation.

The cavitation is not modeled. Therefore, its influence on efficiency is not considered. Areas of low pressure where cavitation could occur are monitored and evaluated through the Sigma coefficient.

The structured computational mesh was created in Ansys Turbogrid for blade passages and ICEM CFD for the draft tube and spiral casing (later used for detailed computations). Figure 6 shows the results of the mesh sensitivity analysis. It shows a loss of accuracy, but the design comparison is adequate.

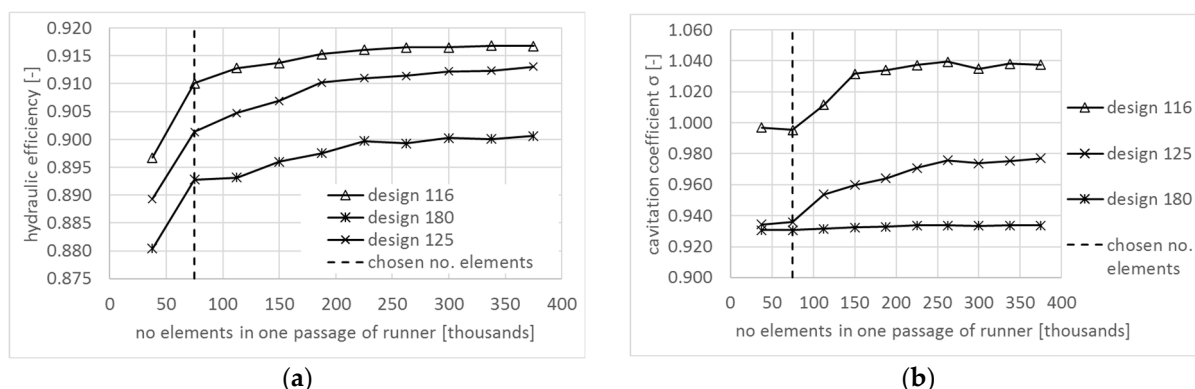


Figure 6. The mesh sensitivity: (a) hydraulic efficiency; (b) cavitation coefficient σ .

Here, more emphasis was placed on limiting the computation time as the amount of computation performed was significant (including many dead ends). The knowledge gained in this work (appropriate procedure, consideration of the influence of the T/l parameter) reduces the number of calculations needed and allows us to choose higher accuracy.

Table 1 shows that although the used computational mesh is relatively coarse, the recommended values of y^+ for the Wall Function are kept. This simplified model is only partially reliable for determining the overall efficiency value [26], but it reliably compares different designs and therefore is suitable for optimization.

Table 1. Computational domains.

Domain	n. of Elem. ¹	y^+ min ¹	y^+ mean ¹	y^+ max ¹
Stator passage	30,720	131	108	144
Guide-vane passage ²	54,672	21	110	252
Runner blade passage	72,480	10	46	116
Draft tube	201,856	33	62	132

¹ Values can vary slightly between the design due to shape and discharge differences. The values shown correspond to the selected candidate. ² The number of elements is higher to obtain satisfying mesh quality for all guide vanes positions.

It is necessary to be aware of the loss of accuracy. Therefore, not one but several candidates are selected on the basis of the optimization process. A detailed analysis of an entire turbine, as described in Section 3.3, verifies the design's performance in the whole operation range.

2.4.3. Optimization Process

Tiwari [27] gives an overview of the use of CFD-based optimization for hydraulic turbine design, which is possible thanks to the increasing computational power and the development of numerical methods. Various optimization approaches have been presented for the Francis turbine [28,29], Kaplan turbine [30], and small hydro turbines [22,31].

The process of optimizing a variable-speed turbine is described in a few publications. The article from NTNU Trondheim [32] details the design of a Francis turbine using a fully parameterized model in Matlab and Ansys CFX. The optiSlang program provides the interfacing and optimization process. Iliev [7] states that the detailed geometry of the entire turbine for optimization can have up to 100 parameters, and performing the sensitivity analysis is recommended to reduce the number of parameters.

In the presented work, the optimization loop is controlled directly from the CAESSES environment using a built-in software connector that provides interfacing. User-defined parameterized scripts manage the whole process and transfer key values (such as the number of elements, iteration time-step, or solver settings) from the CAESSES environment directly to meshing, pre-processing, solver, and post-processing. The obtained results

are also processed in the CAESSES environment. Therefore, the sensitivity analysis and optimization process can be managed directly from CAESSES.

The objective functions for optimization focus on maximizing the efficiency in the Q_{\max} operating point (corresponding with the maximal power output) while maintaining good cavitation properties (Thoma coefficient σ). Determining the cavitation properties of the turbine is based on the static CFD-based evaluation of the pressure distribution on the blades [33]. Thoma's coefficient σ is recalculated to the reference flow rate resulting in σ_{ref} to compare various designs whose flow rates may vary slightly [33].

Initially, optimizing to a weighted average of the efficiencies at three interest operating points (Q_{\min} , Q_{BEP} , and Q_{\max}) was considered. Preliminary calculations have shown that the operating range depends mainly on the relative blade spacing T/l , as described in Section 3.1. Therefore, it was possible to optimize to a single point.

A sensitivity analysis shows how strong the influence of each parameter is on the objective functions. It also helps to find an appropriate range of input parameters. Manual adjustment of the parameter range makes it possible to achieve a suitable design already in this step. Multicriterial optimization by a genetic algorithm (MOGA) can follow. The details of the optimization process are described by Kantor [22]. He also showed that shape optimization could be used to meet specific manufacturing requirements while maintaining hydraulic efficiency.

3. Results

3.1. Design to Maximize the Variable—Speed Operation Range

Farell [9] stated the assumption that turbines with lower relative blade spacing T/l (more or longer blades) would have better characteristics for variable-speed operation. Our preliminary calculations confirmed this assumption. Therefore, it was decided to verify the effect of the T/l ratio on the operation range of variable-speed turbines.

Three turbine designs with various T/l ratios, shown in Figure 7, were assessed by CFD to verify the influence of the T/l ratio t . All designs have a $Q_{11 \text{ BEP}} = 1.6 \text{ m}^3/\text{s}$ ($\pm 5\%$), which corresponds to the designed SHPP Podhora turbine and hydraulic efficiency in the BEP higher than 90% (based on the simplified CFD model as described in Section 2.4.2). Details are provided in Table 2. The complete characteristics of the turbines were calculated from about 200 combinations of runner rotational speed and guide-vanes position. The variable-speed efficiency ridge was extracted from the characteristic.

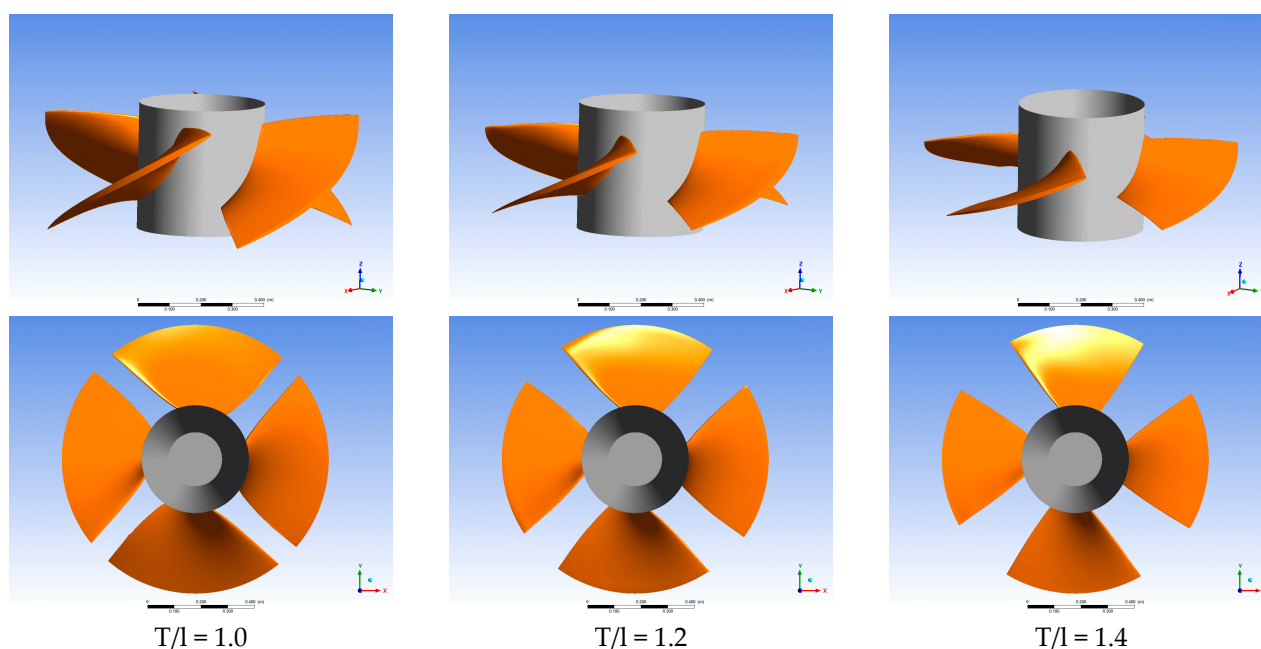


Figure 7. Designs for testing the influence of the T/l ratio on the variable-speed operation range.

Table 2. Test designs with various relative blade spacing T/l .

T/l	$Q_{11 \text{ BEP}}$ [m^3/s]	$n_{q \text{ BEP}}$ [rpm]	η_{BEP} [-]	$Q_{11 \text{ max}}$ [m^3/s]	$P_{11 \text{ max}}$ [kW]
1.0	1.64	163	90.2%	2.57	18.8
1.2	1.58	167	90.3%	2.53	19.1
1.4	1.54	185	90.7%	2.24	17.4

The variable-speed characteristics shown in Figure 8 confirm the initial assumption for flow rates below Q_{BEP} . There is a noticeable difference in the efficiency between the different designs of more than 5% for $0.7 Q_{\text{BEP}}$ and 20% for $0.2 Q_{\text{BEP}}$. For the flow rates higher than Q_{BEP} , there is no significant difference between the designs.

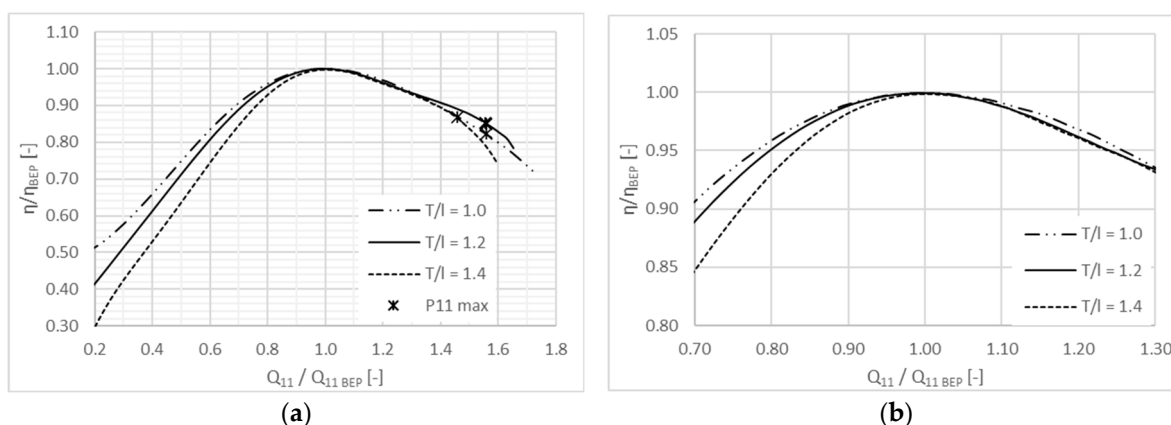


Figure 8. The best efficiency ridge for the variable-speed operation. (a) Operating range from the minimal to maximal flow rate (corresponding with the minimal and maximal power output). (b) Detail in the proximity to the best efficiency point.

The results are convincing. The relative blade pitch $T/l = 1.1$ was chosen for the Podhora SHPP design. Further investigation is needed to generalize these findings and rule out the influence of the design approach.

3.2. Proof of the Concept—Highly Restricted Space Applications—SHPP Podhora

The viability of the proposed workflow was confirmed on the prototype designed for an atypical location where the proposed approach is beneficial. This chapter presents a turbine unit installed on the earth-filled dam's bottom outlets that uses the ecological flow's potential.

The previously proposed conventional design included two PAT turbines. The concept was not cost-effective mainly due to the high powerhouse construction cost compared with annual production. In order not to interfere with existing civil engineering structures, an atypical design was proposed. The turbine, generator, electrical part, and all other related equipment fit into the existing small underground chamber of the dam bottom outlets.

Design parameters based on the described constraints:

- Design head 7.5 m;
- Regulation range $0.70\text{--}0.35 \text{ m}^3/\text{s}$;
- Runner diameter 0.27 m;
- Maximum hydraulic power 20 kW;
- Maximum shaft torque 160 Nm;
- Design speed 1500 rpm;
- Operating speed range 600–1800 rpm;
- Four-pole induction generator.

The design constraints in the form of restricted space and a small chamber entrance ($750 \times 950 \text{ mm}$) limited the runner diameter and significantly influenced the design of the

spiral casing. The tailor-made optimized runner compensated for the negative effect of the constrained hydraulic profile.

The extensive sensitivity analysis allowed us to reduce the number of optimization parameters. Figure 9a shows the hydraulic efficiency of the designs generated during the sensitivity analysis and optimization. Only designs within the acceptable flow range were considered.

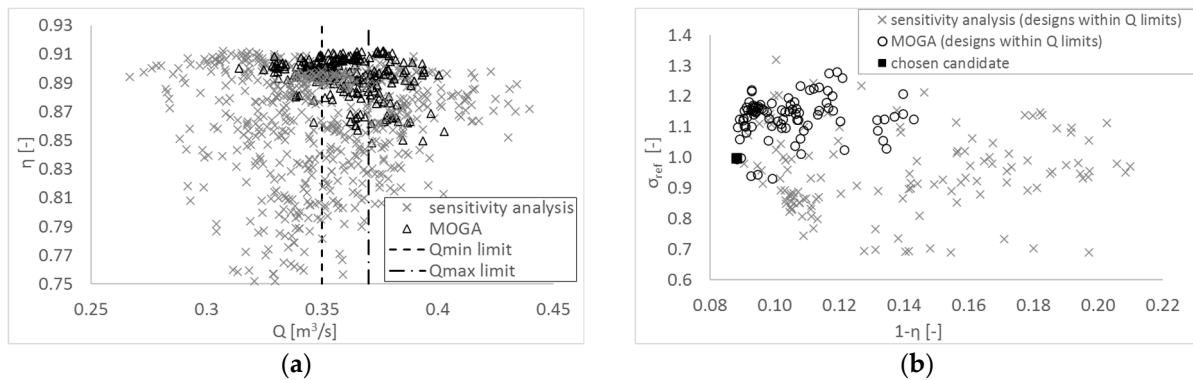


Figure 9. Design and optimization process. (a) Designs generated during sensitivity analysis and optimization; acceptable flow range for considered operating point is indicated. (b) Optimization to two objective functions, only designs with acceptable flows are considered; the graph clearly shows the pareto front of this optimization.

The multi-objective optimization on two objective functions using a built-in Dakota optimizing engine was used to adjust the blade shape and improve two objective functions—the turbine’s efficiency and the value of the cavitation coefficient σ . The global optimization with five design parameters was performed. The properties of the chosen candidate, highlighted in Figure 9b, were further assessed to verify the expected operating range and other characteristics. Figure 10 shows the comparison of the mechanical design model and final realization on site.

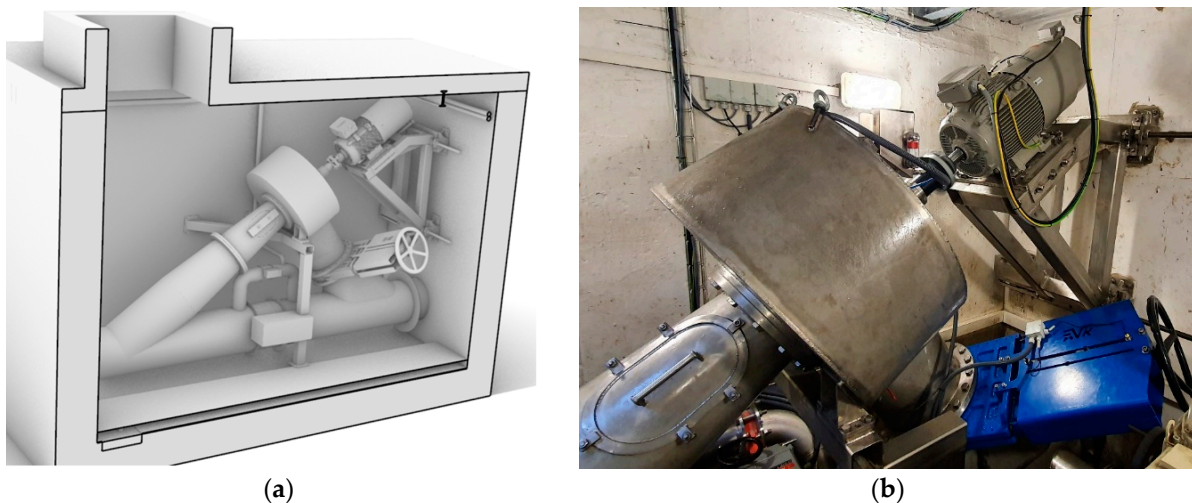


Figure 10. Small HPP Podhora: (a) tailor-made concept that fits into the existing chamber; (b) final realization on-site.

3.3. Turbine Characteristics

Once the design candidate is selected, previous simplified calculations must be verified, and the design behavior over the entire operating range is assessed. The complex steady-state model the entire geometry, including the spiral casing, all blades (10 stator blades, 15 guide vanes, and 4 runner blades), and draft tube, as shown in Figure 5b. The fine

computational grid is used with about 207 thousand elements in one passage of the runner. The process is managed from the CAESSES environment by varying the guide vane's position and the rotational speed while keeping the chosen design of the runner.

The resulting turbine characteristics are constructed from approximately 100 operating points (a combination of the guide vane's position and operation speed) using an in-house previously developed script [34,35] prepared in MatLab[®]. In the first step, the data are recalculated to unit parameters and processed into universal characteristics, as shown in Figure 11. Other scripts follow this processing to construct operating characteristics for both the variable-speed and fixed-speed variants, as shown in Figure 3.

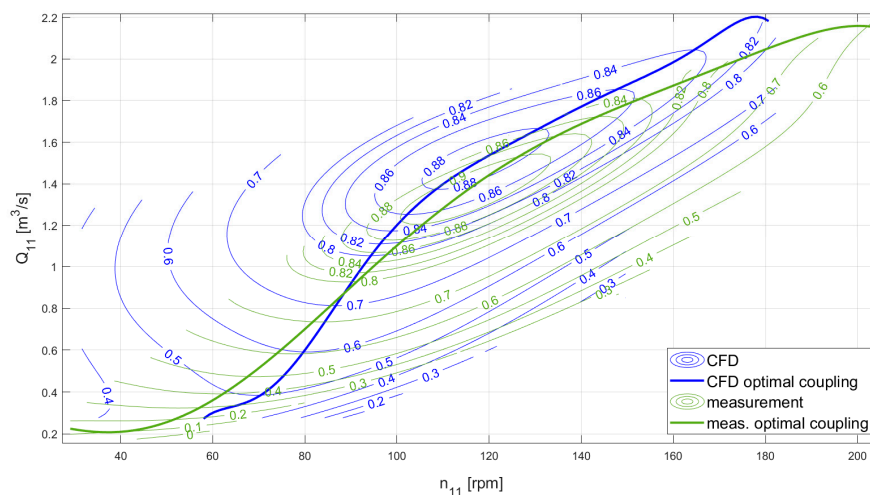


Figure 11. The comparison of CFD calculation and on-site measurement (the universal characteristic).

After the turbine installation, an on-site measurement verified the characteristics of the turbine. The power output, head, and discharge were measured following the norm IEC 62006 [36]. Two relative pressure gauges measured the head—the first was placed in the inlet profile section, and the second was near the end profile of the draft tube. The discharge was calculated from a Poncelet overflow at the end of the stilling basin. A submersible pressure sensor measured the overflow height. Power output was measured only on the electrometer, not directly on the shaft.

Unfortunately, under existing conditions, it was not possible to make better measurements that would have provided a more accurate measurement of the flow and efficiency of the generator with the inverter. Therefore, the re-calculation of the hydraulic efficiency (Figure 11) is affected by error when using the manufacturer's stated efficiencies for the generator, frequency converter, and EMC filter.

Despite the above, the measured values are consistent with the outputs from the CFD model. On-site measurement showed higher efficiency with lower discharge. This may be due to a systematic error in the flow measurement.

4. Conclusions

The concept of the tailor-made axial turbine with adjustable guide vanes and variable-speed regulation was presented. Varying the rotational speed improves adaptation to changing head and discharge and increases overall efficiency. The simplified mechanical design and easy adjustment to a wide range of civil engineering structures make this concept ideal for refurbishing existing power plants. The optimized runner compensates for the compromises made concerning the hydraulic profile. It allows the realization of sites where the conventional solution is not economically viable.

The presented method results in the design with higher efficiency, wider regulation range, reduced cavitation, and lower cost of the civil engineering part compared to the conventional technical solution—in the case of Podhora SHPP, two PAT units in the new

machine room. Once the parametric model with the optimization engine is prepared, it can be used repeatedly, and the time needed for a tailor-made design significantly shortens.

The main conclusions regarding the presented technical concept are as follows:

- Double-regulated variable-speed propeller turbine is highly suitable for small hydro applications. It reduces the investment and maintenance costs while keeping the benefits of double regulation;
- The data confirms Farrell et al.'s [16] assumption that the lower the relative blade spacing T/l , the greater the discharge change with varying speed and the higher benefit of the variable speed. Further investigation on this topic is necessary to exclude the influence of the specific blade design used.

The main conclusions regarding the presented tailor-made design concept are as follows:

- The tailor-made design significantly decreases or even eliminates the civil engineering part costs;
- The tailor-made design enables us to reach high efficiency also for small and very atypical turbines;
- Once the optimization engine and software connection are ready, the time needed for a tailor-made solution decreases significantly;
- Shape optimization is still computationally demanding. The possibility of using surrogate models should be studied.

Author Contributions: Conceptualization, M.K., R.K. and P.N.; data curation, E.B. and R.K.; formal analysis, J.S.; funding acquisition, M.K.; investigation, E.B.; methodology, M.K. and E.B.; project administration, M.K.; resources, M.K.; supervision, P.N.; validation, E.B., J.S. and R.K.; visualization, E.B. and J.S.; writing—original draft, E.B.; writing—review and editing, J.S. and P.N. All authors have read and agreed to the published version of the manuscript.

Funding: This research was funded by TECHNOLOGY AGENCY OF THE CZECH REPUBLIC, grant number TH04010140. The APC was funded by the Department of Hydraulic Structures, Faculty of Civil Engineering, CTU in Prague.

Data Availability Statement: No new data were created or analyzed in this study. Data sharing is not applicable to this article.

Conflicts of Interest: The authors declare no conflict of interest. The funders had no role in the design of the study; in the collection, analyses, or interpretation of data; in the writing of the manuscript; or in the decision to publish the results.

References

1. Farfan, J.; Breyer, C. Aging of european power plant infrastructure as an opportunity to evolve towards sustainability. *Int. J. Hydrogen Energy* **2017**, *42*, 18081–18091. [\[CrossRef\]](#)
2. Kougias, I.; Aggidis, G.; Avellan, F.; Deniz, S.; Lundin, U.; Moro, A.; Muntean, S.; Novara, D.; Perez-Diaz, J.; Quaranta, E.; et al. Analysis of emerging technologies in the hydropower sector. *Renew. Sustain. Energy Rev.* **2019**, *113*, 109257. [\[CrossRef\]](#)
3. Binama, M.; Su, W.-T.; Li, X.-B.; Li, F.-C.; Wei, X.-Z.; An, S. Investigation on pump as turbine (pat) technical aspects for micro hydropower schemes: A state-of-the-art review. *Renew. Sustain. Energy Rev.* **2017**, *79*, 148–179. [\[CrossRef\]](#)
4. Quaranta, E.; Revelli, R. Gravity water wheels as a micro hydropower energy source: A review based on historic data, design methods, efficiencies and modern optimizations. *Renew. Sustain. Energy Rev.* **2018**, *97*, 414–427. [\[CrossRef\]](#)
5. Simmons, S.C.; Lubitz, W.D. Archimedes screw generators for sustainable micro-hydropower production. *Int. J. Energy Res.* **2021**, *45*, 17480–17501. [\[CrossRef\]](#)
6. Valavi, M.; Nysveen, A. Variable-speed operation of hydropower plants. *IEEE Ind. Appl. Mag.* **2018**, *24*, 18–27. [\[CrossRef\]](#)
7. Iliev, I.; Trivedi, C.; Dahlhaug, O.G. Variable-speed operation of francis turbines: A review of the perspectives and challenges. *Renew. Sustain. Energy Rev.* **2019**, *103*, 109–121. [\[CrossRef\]](#)
8. Iliev, I.; Tengs, E.O.; Trivedi, C.; Dahlhaug, O.G. Optimization of francis turbines for variable speed operation using surrogate modeling approach. *J. Fluids Eng.* **2020**, *142*, 101214. [\[CrossRef\]](#)
9. Farrell, C.; Gulliver, J. Hydromechanics of variable speed turbines. *J. Energy Eng.* **1987**, *113*, 1–13. [\[CrossRef\]](#)
10. Borkowski, D.; Wegiel, T. Small hydropower plant with integrated turbine-generators working at variable speed. *IEEE Trans. Energy Convers.* **2013**, *28*, 452–459. [\[CrossRef\]](#)

11. Borkowski, D.; Majdak, M. Small hydropower plants with variable speed operation—an optimal operation curve determination. *Energies* **2020**, *13*, 6230. [[CrossRef](#)]
12. Barsi, D.; Fink, R.; Odry, P.; Ubaldi, M.; Zunino, P. Flow regulation of low head hydraulic propeller turbines by means of variable rotational speed: Aerodynamic motivations. *Machines* **2023**, *11*, 202. [[CrossRef](#)]
13. Europe, M. and R. 3D. Rhino 3d. Available online: <https://www.rhino3d.com/> (accessed on 10 February 2023).
14. Drtina, P.; Sallaberger, M. Hydraulic turbines—Basic principles and state-of-the-art computational fluid dynamics applications. *Proc. Inst. Mech. Eng. Part C J. Mech. Eng. Sci.* **1999**, *213*, 85–102. [[CrossRef](#)]
15. Iman-Eini, H.; Frey, D.; Bacha, S.; Boudinet, C.; Schanen, J.L. Evaluation of loss effect on optimum operation of variable speed micro-hydropower energy conversion systems. *Renew. Energy* **2019**, *131*, 1022–1034. [[CrossRef](#)]
16. Biner, D.; Hasmatuchi, V.; Violante, D.; Richard, S.; Chevailler, S.; Andolfatto, L.; Avellan, F.; Munch, C. Engineering & performance of duoturbo: Microturbine with counter-rotating runners. In *IOP Conference Series: Earth and Environmental Science*; IOP Publishing: Bristol, UK, 2016; Volume 49. [[CrossRef](#)]
17. Vagnoni, E.; Andolfatto, L.; Richard, S.; Munch-Alligne, C.; Avellan, F. Hydraulic performance evaluation of a micro-turbine with counter rotating runners by experimental investigation and numerical simulation. *Renew. Energy* **2018**, *126*, 943–953. [[CrossRef](#)]
18. Nechleba, M. *Vodní Turbíny, Jejich Konstrukce a Příslušenství*; Státní Nakladatelství Technické Literatury: Praha, Czech Republic, 1953; 548p.
19. Caeses Software. Friendship Systems. Available online: <https://www.caeses.com/> (accessed on 19 January 2023).
20. Nikolopoulos, L.; Boulougouris, E. A novel method for the holistic, simulation driven ship design optimization under uncertainty in the big data era. *Ocean Eng.* **2020**, *218*, 107634. [[CrossRef](#)]
21. Priftis, A.; Boulougouris, E.; Turan, O.; Papanikolaou, A. Parametric design and multi-objective optimisation of containerships. *Ocean Eng.* **2018**, *156*, 347–357. [[CrossRef](#)]
22. Kantor, M.; Chalupa, M.; Soucek, J.; Bilkova, E.; Nowak, P. Application of genetic algorithm methods for water turbine blade shape optimization. *Manuf. Technol.* **2020**, *20*, 453–458. [[CrossRef](#)]
23. Kyriacou, S.A.; Weissenberger, S.; Grafenberger, P.; Giannakoglou, K.C. Optimization of hydraulic machinery by exploiting previous successful designs. In *IOP Conference Series: Earth and Environmental Science, Proceedings of the 25th IAHR Symposium on Hydraulic Machinery and Systems, Politehnica Univ Timisoara, Timisoara, Romania, 20–24 September 2010*; IOP Publishing: Bristol, UK, 2010; Volume 12. [[CrossRef](#)]
24. Menter, F.R. 2-equation eddy-viscosity turbulence models for engineering applications. *AIAA J.* **1994**, *32*, 1598–1605. [[CrossRef](#)]
25. Petit, O.; Mulu, B.; Nilsson, H.; Cervantes, M. Comparison of numerical and experimental results of the flow in the u9 kaplan turbine model. In *IOP Conference Series: Earth and Environmental Science, Proceedings of the 25th IAHR Symposium on Hydraulic Machinery and Systems, Politehnica Univ Timisoara, Timisoara, Romania, 20–24 September 2010*; IOP Publishing: Bristol, UK, 2010; Volume 12. [[CrossRef](#)]
26. Jost, D.; Skerlavaj, A.; Lipej, A. Improvement of efficiency prediction for a kaplan turbine with advanced turbulence models. *Stroj. Vestn. J. Mech. Eng.* **2014**, *60*, 124–134. [[CrossRef](#)]
27. Tiwari, G.; Kumar, J.; Prasad, V.; Patel, V.K. Utility of cfd in the design and performance analysis of hydraulic turbines—A review. *Energy Rep.* **2020**, *6*, 2410–2429. [[CrossRef](#)]
28. Kawajiri, H.; Enomoto, Y.; Kurosawa, S. Design optimization method for francis turbine. In *IOP Conference Series: Earth and Environmental Science, Proceedings of the 27th IAHR Symposium on Hydraulic Machinery and Systems (IAHR), Montreal, Canada, 22–24 September 2014*; IOP Publishing: Bristol, UK, 2014; Volume 22. [[CrossRef](#)]
29. Obrovsky, J.; Zouhar, J. Experiences with the hydraulic design of the high specific speed francis turbine. In *IOP Conference Series: Earth and Environmental Science, Proceedings of the 27th IAHR Symposium on Hydraulic Machinery and Systems (IAHR), Montreal, Canada, 22–24 September 2014*; IOP Publishing: Bristol, UK, 2014; Volume 22. [[CrossRef](#)]
30. Abbas, A.I.; Qandil, M.D.; Al-Haddad, M.; Amano, R.S. Investigation of horizontal micro kaplan hydro turbine performance using multi-disciplinary design optimization. *J. Energy Resour. Technol. Trans.* **2020**, *142*, 052101. [[CrossRef](#)]
31. Woldemariam, E.T.; Lemu, H.G.; Wang, G.G. Cfd-driven valve shape optimization for performance improvement of a micro cross-flow turbine. *Energies* **2018**, *11*, 248. [[CrossRef](#)]
32. Tengs, E.; Storli, P.T.; Holst, M. Optimization procedure for variable speed turbine design. *Eng. Appl. Comput. Fluid Mech.* **2018**, *12*, 652–661. [[CrossRef](#)]
33. Benigni, H.; Montenari, B.; Jaberg, H.; Schiffer, J.; Gehrler, A.; Grundner, F.; Dörlmayer, R. Simulation of damages due to cavitation in non- rotating components in a kaplan turbine. In *Proceedings of the 19th Internationales Seminar Wasserkraftanlagen*, Vienna, Austria, 9–11 November 2016.
34. Karbulka, D. Model and Operational Characteristics of Axial Turbine. Bachelor’s Thesis, Czech Technical University, Prague, Czech Republic, 2020. Volume 56.
35. Karbulka, D. Optimization of Axial Turbine Unit Parameters. Master’s Thesis, Czech Technical University, Prague, Czech Republic, 2021. Volume 55.
36. *IEC 62006:2010; Hydraulic Machines—Acceptance Tests of Small Hydroelectric Installations*. IEC: Geneva, Switzerland, 2010; p. 223.

Disclaimer/Publisher’s Note: The statements, opinions and data contained in all publications are solely those of the individual author(s) and contributor(s) and not of MDPI and/or the editor(s). MDPI and/or the editor(s) disclaim responsibility for any injury to people or property resulting from any ideas, methods, instructions or products referred to in the content.